Limnol. Oceanogr., 48(5), 2003, 1846–1854

The balance between silica production and silica dissolution in the sea: Insights from Monterey Bay, California, applied to the global data set

Mark A. Brzezinski[1] *and Janice L. Jones*
Marine Science Institute and Department of Ecology, Evolution, and Marine Biology, University of California, Santa Barbara, California 93106

Kay D. Bidle[2] *and Farooq Azam*
Marine Biology Research Division 0202, Scripps Institution of Oceanography, University of California San Diego, La Jolla, California 92093

Abstract

Silicon isotope tracers were used to examine the relative magnitude of silica dissolution and silica production in the Monterey Bay, California, upwelling system. A diatom bloom dominated by *Skeletonema costatum* and *Chaetoceros* spp. was encountered under conditions of moderate upwelling. Profiles of silica production and dissolution rates were obtained at seven stations that sampled both inside and outside the bloom. Integrated silica production rates ranged from 5.4 to 108 mmol Si m^{-2} d^{-1}, averaging 42.8 mmol Si m^{-2} d^{-1}. Integrated silica dissolution rates were considerably lower than production rates with values between 0.63 and 6.5 mmol Si m^{-2} d^{-1} (mean = 2.90 mmol Si m^{-2} d^{-1}). The mean ratio of integrated silica dissolution to integrated silica production ($\int D : \int P$) between the surface and the 0.1% light depth was 0.075, omitting one station with an unusually high $\int D : \int P$ of 0.61, indicating that, on average, 93% of silica production was supported by new silicic acid. The *f*-ratio for diatom nitrogen use estimated from silicic acid and nitrate depletion curves and the mean $\int D : \int P$ ratio was found to be 0.83, indicating that silica was being regenerated at a rate that was only slightly slower than that for particulate organic nitrogen. These data provide direct evidence confirming earlier hypotheses that the silica pump is weak in Monterey Bay. Analysis of the global data set on $\int D : \int P$ in the surface ocean leads to the hypothesis that low $\int D : \int P$ (~0.10 or less) are typical of diatom bloom events, with $\int D : \int P$ rising to values in excess of 0.50 during nonbloom periods. This pattern is shown to be consistent with previous estimates that the annual mean $\int D : \int P$ ratio in the upper 200 m of the global ocean is 0.5–0.6. A regional analysis reveals that the fraction of silica production supported by new silicic acid varies as a hyperbolic function of the level of gross silica production similar to the variation in the *f*-ratio for N use with primary productivity. These trends suggest that diatom blooms, especially those occurring in more productive waters, are the main vectors of silica export in the sea, with the majority of the silica produced during nonbloom periods being recycled in the euphotic zone.

The relative rates at which silica and organic matter are recycled in the euphotic zone determine whether diatom-dominated pelagic ecosystems are driven to silicon or nitrogen limitation. Dugdale et al. (1995) formalized this concept in what they termed the ''silicate pump.'' In their model, grazing and remineralization processes in the euphotic zone tend to recycle organic matter more rapidly than they do particulate silica, causing sinking particles to be enriched in Si over N compared to the relative rates at which particulate organic nitrogen (PON) and biogenic silica ($bSiO_2$) are produced. Thus, the biological pump removes $bSiO_2$ from the euphotic zone with greater efficiency than it does PON, with the ultimate result that the system is driven toward Si limitation. Here, we use the terminology ''silica pump'' rather than the term ''silicate pump'' because it is biogenic silica, not dissolved silicon, that is exported (i.e., pumped) from the surface ocean to depth. The silica pump seems especially strong in high nutrient–low chlorophyll areas (Dugdale et al. 1995; Dugdale and Wilkerson 1998; Brzezinski et al. 2001), but it has not been evaluated extensively in other regions of the ocean.

The balance between integrated silica production and integrated silica dissolution in the euphotic zone, which we term the integrated dissolution to production rate ratio ($\int D : \int P$), is a key determinant of the strength of the silica pump. When the quantity $1 - \int D : \int P$ (i.e., the fraction of silica production supported by new silicic acid, $Si(OH)_4$) is greater than the *f*-ratio for nitrogen use, $bSiO_2$ is being recycled to a lesser extent than is PON, driving the system to Si limitation. Conversely, when $1 - \int D : \int P$ is less than the *f*-ratio, silica is being recycled at a greater rate than is PON, and N limitation is favored. Although the *f*-ratio has been evaluated in a wide variety of environments (e.g., Eppley and Peterson 1979), estimates of $\int D : \int P$ in the surface ocean are few (*see* summary by Nelson et al. 1995). Only eight studies have evaluated the magnitude of $\int D : \int P$ for the euphotic zone (*see* Nelson et al. 1995; Brzezinski et al. 2001). Despite the scarcity of data, the range of observed values of $\int D : \int P$ spans an order of magnitude, with values as low as 0.1 and others that exceed 1.0 (Nelson et al. 1995; Brzezinski et al. 2001). The implication is that there is a high degree of variability in the extent of silica recycling in the surface ocean.

[1] Corresponding author (brzezins@lifesci.ucsb.edu).
[2] Present address: Institute of Marine and Coastal Science, Rutgers University, 71 Dudley Road, New Brunswick, New Jersey 08901.

Acknowledgments

We thank the captain and crew of the R/V *Point Sur* for their help and cooperation at sea. This research was supported by NSF grant OCE-9904410 to M.A.B. and OCE-9819603 to F.A.

The magnitude and variability of $\int D : \int P$ in different regions of the surface ocean is one of the greatest uncertainties in the global marine silica budget. Nelson et al. (1995) examined the available data and found a mean $\int D : \int P$ to be 0.58. They used an estimated global mean $\int D : \int P$ value of 0.5 to convert their estimate of global gross silica production of 200–280 Tmol Si yr^{-1} (1 Tmol = 1×10^{12} mol) to a net silica production of 100–140 Tmol Si yr^{-1}. Using a global circulation modeling (GCM) approach, Gnanadesikan (1999) and Gnanadesikan and Toggweiler (1999) argued that global net production could be no more than 90 Tmol Si yr^{-1}. Reconciling that estimate with that of Nelson et al. (1995) requires an upward adjustment of the global mean $\int D : \int P$ value used by Nelson et al. (1995) from 0.50 to 0.64, which is well within present levels of uncertainty in the ratio.

One important consistency arising from the studies of Nelson et al. (1995), Gnanadesikan (1999), and Gnanadesikan and Toggweiler (1999) is that the mean $\int D : \int P$ ratio in the surface ocean is at least 0.5, implying that half or more of all marine silica production is supported by the $Si(OH)_4$ that is recycled within the euphotic zone. This means that the silica cycle of the near-surface ocean has at least as many similarities to that of a highly regenerated nutrient, like ammonium, as it does to a largely ''new'' nutrient, like nitrate (Brzezinski and Nelson 1989). Despite the importance of silica dissolution in regenerating $Si(OH)_4$ in the surface ocean, great uncertainty remains regarding the factors controlling the temporal and spatial variability in the $\int D : \int P$ ratio in different regions of the global ocean and the influence that this variation has on phytoplankton dynamics, the silica cycle, and the links between the silica cycle and organic matter production and export.

The mechanisms influencing dissolution in surface waters are known in only the most general of terms. Seawater is everywhere undersaturated with $Si(OH)_4$ (Hurd 1972), causing any biogenic silica surface that is exposed to seawater to undergo chemical dissolution. The rate of dissolution is known to be dependent on temperature (Kamatani and Riley 1979; Kamatani 1982) and the surface area of the dissolving silica (e.g., Hurd and Birdwhistell 1983). The organic coating that surrounds living diatoms deters dissolution, and its removal accelerates dissolution dramatically (Kamatani 1982). Recent laboratory studies have shown that degradation of the organic matter surrounding diatom frustules by natural assemblages of marine bacteria greatly accelerates silica dissolution, providing the first direct demonstration of a biological process that can affect diatom dissolution rates in the sea (Bidle and Azam 1999, 2001). Moreover, new field experiments have now for the first time demonstrated the role of bacterial protease activity in accelerating silica dissolution rates in situ (Bidle et al. 2003).

In the present study, we use spatial gradients in diatom biomass and silica production in a temperate coastal upwelling system to further examine trends in $\int D : \int P$ within natural diatom assemblages. The values of $1 - \int D : \int P$ obtained were only slightly greater than estimates of the *f*-ratio for diatom N use in Monterey Bay, confirming that the silica pump is weak in this system. Comparison of the results from Monterey Bay with other regional estimates of $1 - \int D : \int P$ reveals a systematic change in the ratio as a function of gross silica production.

Methods

A rosette system equipped with 10-liter Niskin bottles fit with silicone springs and a Sea-Bird CTD was used to collect samples from the upwelling zone near Monterey Bay, California. A survey grid of 19 stations was occupied from 10–20 April 2000 (Fig 1). Water samples were collected from 5 m at all grid stations. Immediately following the survey grid, profiles of water column properties were obtained at 10 stations selected to encompass a range of physical and biological conditions (Fig. 1). The water column was sampled at six depths corresponding to 100, 54, 16, 3.6, 0.6, and 0.1% of the irradiance just below the sea surface (E_o). Profiles extended from the surface to between 20 and 80 m depending on water clarity. Each Niskin bottle was drained in its entirety into a 10-liter polypropylene carboy shielded with black plastic and mixed to homogenize the particles. All samples were drawn from the carboys.

The concentrations of $Si(OH)_4$ and $bSiO_2$ were determined at all stations. Samples for $[Si(OH)_4]$ were collected in polypropylene bottles and analyzed in duplicate using the method described by Brzezinski et al. (2001), which has a detection limit of 0.05 μmol L^{-1}. Samples for $[bSiO_2]$ analysis were drained into 320-ml polypropylene bottles and then processed at sea as described by Brzezinski et al. (2001). Back in the laboratory, the biogenic silica was analyzed using a NaOH digestion technique that has a precision of 10% (Brzezinski et al. 2001).

Silica production rates were determined using the radioisotope ^{32}Si (Los Alamos National Laboratory), specific activity = 20,000 Bq $(\mu g\ Si)^{-1}$. Stock solutions of the radioisotope were cleaned of trace metals by passage through Chelex resin prior to use. Seawater subsamples for silica production rate determination were drained into 280-ml acid-cleaned polycarbonate bottles. Then ~1,800 Bq of the ^{32}Si tracer solution was added. The addition of the tracer increased ambient $[Si(OH)_4]$ by 12 nmol Si L^{-1}. The samples were incubated on deck in an acrylic incubator equipped with neutral density screens that reproduced in situ light intensities at the depth of collection (0.1–100% E_o). Flowing surface seawater was used to maintain temperature. At the end of the incubation, the particulate material in each sample was collected and assayed for ^{32}Si activity by liquid scintillation counting as described by Brzezinski and Phillips (1997). Typical counting precision was 1–2% (±2 SD). Samples for production rate measurements on the survey grid were incubated for 24 h to eliminate time of day as a factor influencing rates obtained among stations. Incubations at each profile station lasted 4–6 h. Previous time course measurements of silica production rate data from Monterey Bay (Brzezinski and Phillips 1997) show a linear increase in silica production with time over 24 h ($R^2 = 0.96$) with a standard deviation of the data about a linear regression line fit to the time course of 10.3%. Absolute silica production rates (ρ, μmol Si L^{-1} d^{-1}) were calculated from the fraction of the tracer taken up and the ambient $[Si(OH)_4]$ as described

by Brzezinski and Phillips (1997). Specific silica production rates normalized to [$bSiO_2$] (V_b) were calculated using the logarithmic equation given by Brzezinski and Phillips (1997). Our analysis of biogenic silica concentration does not distinguish between silica in living diatoms and that in detritus, causing V_b to be conservatively low relative to the activity of living cells. Calculation of ρ is independent of [$bSiO_2$] and thus is not biased by the uncertainty in the biomass of living diatoms.

Silica dissolution rates were measured using the isotope dilution method of Nelson and Goering (1977) modified to use a new simplified procedure to recover dissolved silicon from seawater samples. The recovery method, based on the magnesium-induced coprecipitation (MAGIC) method for phosphate recovery (Karl and Tien 1992), uses the formation of a $Mg(OH)_2$ (brucite) to scavenge $Si(OH)_4$ from the sample. We describe the process in some detail because it is a new methodology for silica dissolution rate measurement.

Acid-cleaned 2.8-liter polycarbonate bottles were used to collect 2.4-liter samples of seawater. To each bottle, 30 μmol of a mixture of ^{29}Si (95.65 atom %) and ^{30}Si (95.28 atom %), 4 : 1 mole ratio, were added. (Note that a mixture of ^{29}Si and ^{30}Si was used as tracer rather than either alone in order to increase the voltage signal from ^{28}Si on our single collector mass spectrometer, which enhances the precision of the measurement.) Following the addition of tracer, each sample was mixed and divided between two 1-liter acid-cleaned polycarbonate bottles. One of each pair of 1-liter bottles was placed in the deck incubators at the appropriate light level for 24 h, whereas the remaining split was processed immediately. Sample processing entailed filtering each sample through a 0.6-μm polycarbonate filter and collecting the filtrate in a 1-liter acid-washed high-density polyethylene bottle. Brucite precipitation was conducted in acid-washed 1-liter polycarbonate settling cones equipped with Teflon stopcocks. Each filtrate was poured into a cone, and 6 ml of 14.8 mol L^{-1} trace metal–grade NH_4OH was added to induce brucite formation. Brucite precipitation is immediate. We substituted NH_4OH for the NaOH used in the original MAGIC method (Karl and Tien 1992) because the precipitate formed with NH_4OH behaved in a more consistent manner during subsequent processing than did that formed with NaOH. Each cone was covered with Parafilm® that had been cleaned with deionized distilled water (DDW). The Parafilm was held in place with a plastic lid. Each cone was inverted several times to ensure thorough mixing. The precipitate was left to settle for 12–24 h, during which time the precipitate was collected at intervals as described below. The volume of NH_4OH required to maximize the recovery of $Si(OH)_4$ varies with the [$Si(OH)_4$] in the sample: recovery is 98% using 6 ml of NH_4OH when [$Si(OH)_4$] is $\leq$25 μM and 97% using 12 ml of NH_4OH when [$Si(OH)_4$] is 70 μmol L^{-1}. Six milliliters of NH_4OH were used in this study.

The brucite was recovered from each settling cone by draining 40-ml aliquots through the stopcock into 50-ml DDW-rinsed polypropylene centrifuge tubes. Each tube was then centrifuged at 1,120 $\times$ g for 10 min, and the supernatant was discarded. A second draw-off of precipitate was done into the same tube, and the contents were resuspended and centrifuged again. Without resuspension, the pellet of precipitate is extremely difficult to dissolve in later processing. The solution in each cone was swirled and allowed to sit a further 6 h before collecting the remaining precipitate. Collection tubes were capped, wrapped in Parafilm, and returned to the laboratory for final processing. After the 24-h incubation period, the second 1-liter bottle of each sample pair was processed in the same manner.

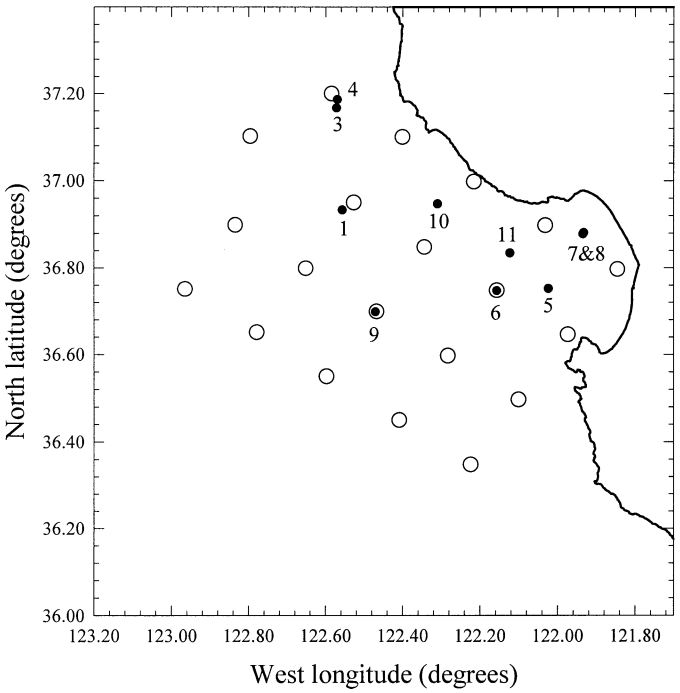

Fig. 1. Locations of stations sampled on the survey grid (open circles) and stations where full profiles (0.1–100% E_o) of properties were obtained (closed circles). Numbers are station numbers for profile stations (*see Table 1*).

The silicon in each tube was converted to $BaSiF_6$ for mass spectrometry. The silicon was first reacted to silicomolybdic acid by reaction with 10 ml of acid molybdate (1 : 2 parts of 1 mol L^{-1} HCl : 0.03 mol L^{-1} $(NH_4)_6Mo_7O_{24}\cdot 4H_2O$) that had been cleaned of Si by the addition of NaCl (25 g L^{-1}) and passage through Sephadex (Brzezinski and Nelson 1986). If necessary, 10 mol L^{-1} HCl was added dropwise to the samples after the addition of the acid-molybdate reagent to attain a pH of between 2 and 3, which favors the formation of silicomolybdic acid. After 60 min, the yellow silicomolybdic acid was concentrated onto a column of Sephadex resin and rinsed with a solution of 0.01 mol L^{-1} HCl/25 g L^{-1} NaCl to remove ions that would later form insoluble salts with barium. The Si on the column was eluted by decomposing the silicomolybdic acid with 2 ml of 1.6 mol L^{-1} NaOH. The eluant was filtered through a 0.2-μm polyvinylidene fluoride syringe filter into a new DDW-rinsed polystyrene tube. The samples were then placed in a vacuum drying oven (65°C, 50 cm Hg vacuum) for volume reduction. When a volume of between 0.75 and 1 ml was obtained, the Si in each tube was precipitated as Na_2SiF_6 by the addition of 500 μl of 30% H_2O_2, 900 μl of 10 mol L^{-1} HCl, and 200 μl of 7.5 mol L^{-1} HF. Attempts to precipitate $BaSiF_6$ rather than Na_2SiF_6 from the reduced solution were unreliable, even

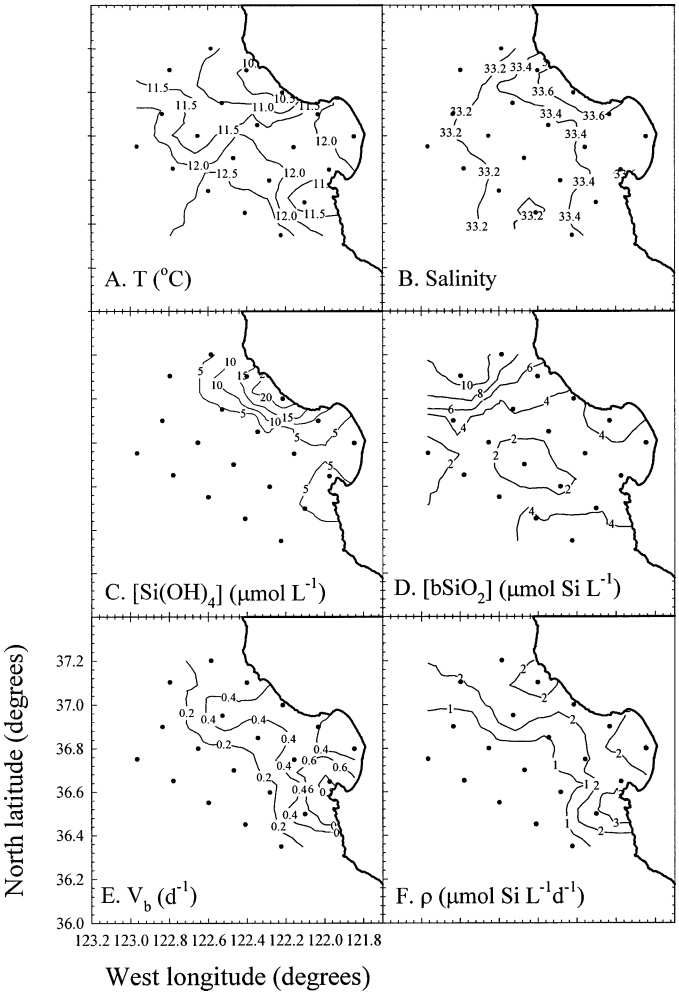

Fig. 2. Contours of (A) temperature, (B) salinity, (C) silicic acid concentration ($[Si(OH)_4]$), (D) biogenic silica concentration ($[bSiO_2]$), (E) specific silica production rates (V_b), and (F) silica production rates (ρ) at 5 m depth.

when salts that did not contain Na were used as reagents. The Na_2SiF_6 was rinsed with methanol and dried in a vacuum drying oven (65°C, 50 cm Hg vacuum). The dried Na_2SiF_6 was dissolved with 0.5 ml of DDW, and the solution was acidified with 670 μl of 10 mol L^{-1} HCl. $BaSiF_6$ was then precipitated by the addition of 200 μl of 2.5 mol L^{-1} HF and 1,000 μl of 1 mol L^{-1} $BaCl_2$. The $BaSiF_6$ was rinsed with methanol, transferred to microcentrifuge tubes, and dried at 60°C overnight in a vacuum oven (50 cm Hg vacuum).

The isotopic composition of the silicon in each sample was determined by solid-phase mass spectrometry using a MAAS 6-60 mass spectrometer with a precision of 1 part in 5,000. Analysis of replicate samples indicate an analytical precision of better than ±5%. Absolute dissolution rates (ρ_{dis}) and specific dissolution rates (V_{dis}) were calculated using the equations of Nelson and Goering (1977). V_{dis} is affected by the relative proportions of living and detrital silica in the samples because living diatoms dissolve at substantially lower rates than detrital silica that is free of organic matter (Nelson et al. 1976; Kamatani and Riley 1979; Kamatani 1982); thus, the reported values of V_{dis} represent the mean rate for siliceous particles (living diatoms and detrital silica). Values of ρ_{dis} are not biased by the inability to separate detrital and living $bSiO_2$.

Results

Survey grid—Low temperature and high salinity revealed the location of upwelled waters along the northwest corner of Monterey Bay (Fig. 2A,B). Silicic acid concentrations were >20 μmol L^{-1} in the upwelled waters, with values of <5 μmol L^{-1} observed over the rest of the Bay and in the offshore waters (Fig. 2C). Siliceous biomass was highest to the north of the Bay, where $bSiO_2$ concentrations in excess of 10 μmol Si L^{-1} were found (Fig. 2D). Microscopic examination of near-surface waters from this area revealed the presence of a bloom of the diatoms *Skeletonema costatum* and *Chaetoceros* spp. that extended to the north toward San Francisco Bay (unpubl. satellite imagery). $bSiO_2$ concentrations were generally <5 μmol Si L^{-1} outside the bloom.

Specific production rates of biogenic silica (V_b) were between 0.4 and 0.6 d^{-1} over much of the study area, corresponding to estimated doubling times for the diatom assemblages of between 1.7 and 2.5 d (Fig. 2E). Higher rates were observed at the south end of the Bay, where apparent doubling times were <1 d. Silica production was greatest nearshore, where values were between 2 and 3 μmol Si L^{-1} d^{-1}. Silica production rates were <1 μmol Si L^{-1} d^{-1} offshore (Fig. 2F).

Profile stations—The locations of stations where full profiles (surface to 0.1% E_o) of properties were obtained are indicated in Fig. 1. These locations were chosen to sample across gradients in diatom biomass and $[Si(OH)_4]$ to investigate how silica dissolution and silica production varied both inside and outside the diatom bloom. Representative profiles are shown in Fig. 3. These stations are aligned approximately from north to south (Fig. 1) and span the strong meridional gradient in siliceous biomass and $[Si(OH)_4]$ measured during the occupation of the grid (Fig. 2). Stations 1 and 3 were located within the diatom bloom and had $[bSiO_2]$ of between 5 and 10 μmol Si L^{-1} and $[Si(OH)_4]$ of <3 μmol L^{-1} in the upper 20 m (Fig. 3). Both $[bSiO_2]$ and $[Si(OH)_4]$ were low at Sta. 9, located just outside of the bloom, where $[Si(OH)_4]$ and $[bSiO_2]$ were ~3 μmol L^{-1} and <1 μmol Si L^{-1}, respectively, throughout the upper water column.

Silica production (ρ) was between 2 and 6 μmol Si L^{-1} d^{-1} in the upper 20 m at the two stations within the bloom (Stas. 1, 3; Fig. 3). Values of ρ outside of the bloom were more than an order of magnitude lower, with a maximum value of 0.1 μmol Si L^{-1} d^{-1}. Specific silica production rates of biogenic silica (V_b) were between 0.2 and ~0.8 d^{-1} in surface waters at all three stations, corresponding to apparent doubling times of 0.9–3.5 d. There was a tendency for the mean V_b in the water column to decrease from the most northern to the most southern station (Fig. 3).

Specific rates of silica dissolution (V_{dis}) were less than 0.06 d^{-1} throughout the upper 30 m at all three stations (Fig. 3). Absolute silica dissolution rates (ρ_{dis}) were generally between 0.2 and 0.7 μmol Si L^{-1} d^{-1} at all three stations.

Values of ρ_{dis} were considerably lower than values of ρ, resulting in silica dissolution : production rate ratios (D : P) measured at a given depth in the water column of ~0.1 or less (Fig. 3). D : P was uniform with depth at Stas. 3 and 1 but increased dramatically with depth at Sta. 9, where D : P increased from <0.05 at the surface to 0.60 at 42 m (the deepest depth sampled).

Integrated properties (surface to the 0.1% light depth) for all profile stations are given in Table 1. Integrated siliceous biomass was between 44 and 175 mmol Si m^{-2}, averaging 105 mmol Si m^{-2}. The mean V_b for each profile indicated doubling times of 1 to ~3.5 d for the overall data set. Integrated rates of silica production averaged 43 mmol Si m^{-2} d^{-1}, with most values <100 and some values <10 mmol Si m^{-2} d^{-1} (Table 1), indicating a modest level of silica production. Integrated dissolution rates were generally much lower than integrated production rates, being between 0.6 and 6.5 and averaging 2.90 mmol Si m^{-2} d^{-1}, resulting in a mean net silica production rate of 35.6 mmol Si m^{-2} d^{-1} (Table 1). On average, the $\int D : \int P$ ratio was 0.151 ± 0.204 (mean ± SD). That value is biased by the one high $\int D : \int P$ value of 0.607 at Sta. 6 (Table 1). Without that value, $\int D : \int P$ averaged 0.075 ± 0.036.

The highest $\int D : \int P$ occurred at Sta. 6, which had low biomass, a low ambient [$Si(OH)_4$], and a low integrated silica production rate, but which had an integrated dissolution rate that was just above the mean for all stations (Table 1). The low [$Si(OH)_4$], low biomass, and low silica production rate at this station suggest the end of a phytoplankton bloom, but there is too little data to confirm this hypothesis.

Discussion

Our study was conducted during a period of modest silica production compared to that observed by Brzezinski et al. (1997) in this same area during a strong upwelling event, when integrated production rates reached 1,140 mmol Si m^{-2} d^{-1} (mean = 205 mmol Si m^{-2} d^{-1}). With all other factors being equal, lower production rates would be expected to favor higher $\int D : \int P$ ratios. This implies that our mean $\int D : \int P$ ratio of <10% might be conservatively low for more intense diatom blooms.

Our mean $\int D : \int P$ value is very close to that observed in Monterey Bay in 1992 ($\int D : \int P = 0.10$, mean of three stations, Brzezinski et al. unpubl. data, cited in Nelson et al. 1995) and is similar to the value of 0.1 estimated indirectly for the coastal upwelling system off Peru (Nelson et al. 1981). It is lower than the $\int D : \int P$ value of ≥1.0 measured in the coastal upwelling system off northwest Africa, where upwelling was scouring frustules from sediments and winds were delivering Saharan dust to the coastal waters (Nelson and Goering 1977). These studies all targeted periods of active upwelling and constitute the current global data set on $\int D : \int P$ ratios for coastal upwelling systems. With the exception of the unusual situation encountered off northwest Africa, the cumulative data set indicates that $\int D : \int P$ is low (~0.1) for diatoms blooming in upwelled waters.

Our measurements allow the first direct assessment of the strength of the silica pump in Monterey Bay. Earlier assessments were made without the benefit of direct measures of silica dissolution rates (Brzezinski et al. 1997). The silica production and dissolution rate data obtained in this study allow a more refined assessment of the strength of the silica pump during a modest upwelling event in this region. On average, the fraction of silica production supported by new silicic acid within the bloom that we sampled was $1 - \int D : \int P = 1 - 0.075 = 0.93$. That value is higher than estimates of the *f*-ratio for coastal upwelling systems that rarely exceed 0.85 (Eppley and Peterson 1979; Dugdale and Wilkerson 1989). The slope of the nitrate and silicic acid depletion curve in the upwelling region of Monterey Bay under diatom-dominated conditions is $\Delta NO_3^- : \Delta Si(OH)_4 = 0.89$ (Brzezinski et al. 1997). Assuming a diatom N : Si ratio of 1 in this Fe-replete region (Bruland et al. 2001) and no silica dissolution, the *f*-ratio for diatom productivity is 0.89. Our data indicate that the assumption that silica does not dissolve in surface waters is false, causing this simple calculation to overestimate the *f*-ratio for diatom N use. This occurs because the N taken up to balance the consumption of regen-

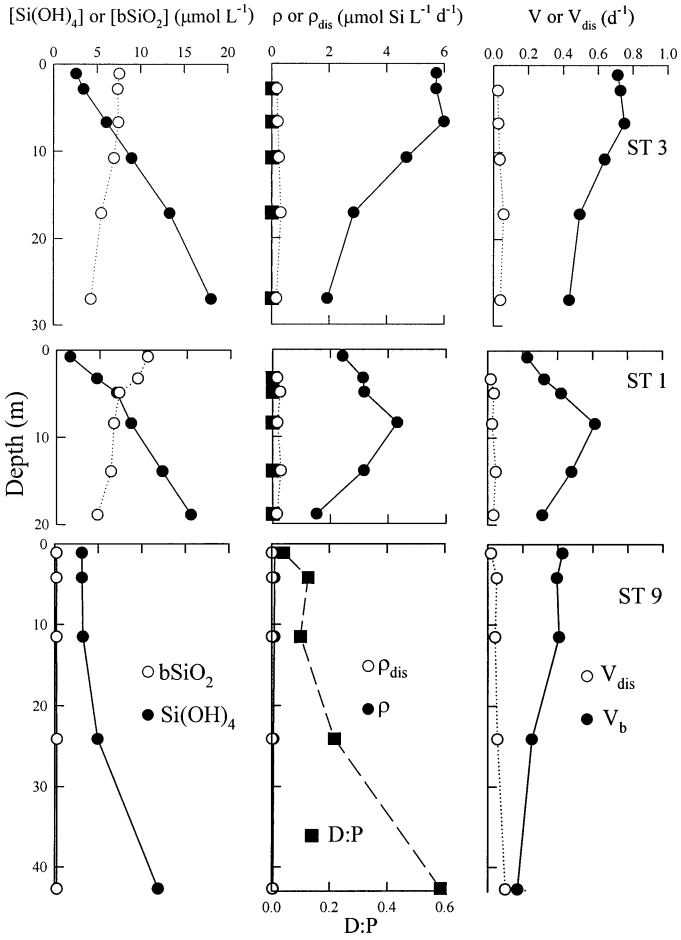

Fig. 3. Representative profiles of silicic acid concentration ([$Si(OH)_4$]) and biogenic silica concentration ([$bSiO_2$]), silica production rates (ρ) and silica dissolution rates (ρ_{dis}), and the specific rates of silica production (V_b) and dissolution (V_{dis}) for three stations. Profiles of the dissolution : production rate ratios (D : P) are also included in the second column of plots for comparison. The locations of Stas. 1, 3, and 9 are given in Fig. 1.

Table 1. Integrated properties for profile stations in Monterey Bay.

Station	$\int bSiO_2$ (mmol Si m^{-2})	$\int \rho$ (mmol Si m^{-2} d^{-1})	$\int \rho_{dis}$ (mmol Si m^{-2} d^{-1})	Net silica production (mmol Si m^{-2} d^{-1})	$\int D : \int P$	Mean V_b (d^{-1})	Doubling time (d)	Mean V_{dis} (d^{-1})
1	134	59.5	4.1	55.4	0.069	0.40	1.7	0.032
3	167	108	6.5	102	0.060	0.63	1.1	0.038
4	175	—	—	—	—	—	—	—
5	109	29.2	2.2	27.0	0.076	0.21	3.4	0.039
6	44.3	5.4	3.3	2.1	0.607	0.19	3.6	0.111
7	107	73.0	—	—	—	0.67	1.0	0.048
8	142	—	—	—	—	—	—	—
9	16.3	4.8	0.63	4.2	0.131	0.35	2.0	0.054
10	104	32.2	2.95	29.2	0.092	0.40	1.7	0.021
11	60.2	30.2	0.65	29.5	0.022	0.55	1.3	0.021
Mean	106	42.8	2.90	35.6	0.151	0.42	2.0	0.045

erated $Si(OH)_4$ in the euphotic zone must come from regenerated N sources in order to maintain the observed slope of the $NO_3^- : Si(OH)_4$ depletion curve. Given a mean $\int D : \int P$ ratio of 0.075, the *f*-ratio for diatom productivity is re-estimated to be $0.89/(1 + 0.075) = 0.83$. That value is lower than the fraction of silica production supported by new silicic acid, 0.93, causing $Si(OH)_4$ to be depleted at a rate that is about 10% faster than that for nitrate in the Monterey Bay region.

This analysis confirms earlier estimates that, although the concept of a silica pump applies to Monterey Bay, the pump is fairly weak during upwelling. Moreover, nitrate rather than silicic acid depletion occurs in the Bay despite the more rapid use of silicic acid compared to nitrate by the phytoplankton. This occurs because upwelling waters in Monterey Bay contain 20–30% more silicic acid than nitrate. The strength of the silica pump is insufficient to overcome that greater supply of $Si(OH)_4$ versus NO_3^- from upwelling, and the system is driven to nitrate depletion, consistent with the conclusion that $Si(OH)_4$ is not a strong regulator of diatom productivity in Monterey Bay (Kudela and Dugdale 2000). These observations reinforce the importance of comparing the strength of the silica pump to the relative supplies of $Si(OH)_4$ and NO_3^- in surface waters when evaluating the effect of the pump on nutrient limitation (Dugdale et al. 2002).

In contrast to coastal environments, high values of $\int D : \int P$ (i.e., 0.6–0.8) have been reported for the oligotrophic open ocean (Brzezinski and Nelson 1995; Nelson and Brzezinski 1997). The large range in $\int D : \int P$ in the global data set inspired us to examine whether $\int D : \int P$ varies in a systematic way relative to silica production. Eight regional estimates are available representing a range of ocean environments, including such widely differing systems as the Sargasso Sea, the Peru upwelling system, and the Antarctic Circumpolar Current (ACC). Two data sets were excluded from the analysis: the study by Nelson and Goering (1977) off northwest Africa and the data from the turbid waters of the Amazon River plume presented by DeMaster et al. (1991). In both studies, the reported $\int D : \int P$ ratios have a high likelihood of reflecting the characteristics of allochthonous silica rather than being representative of the rate of recycling of biogenic silica produced and retained within the euphotic zone. $\int D : \int P$ ratios observed off northwest Africa were ≥ 1 as a result of a net flux of silica into the area via sediment resuspension or wind-borne Saharan dust (Nelson and Goering 1977). In the case of the turbid portions of the Amazon River plume, $\int D : \int P$ ratios would have been influenced by the high load of suspended particulate silica from the river (DeMaster et al. 1991). Data from nonturbid waters in the Amazon plume were included in the analysis.

When the fraction of silica production supported by new silicic acid, $1 - \int D : \int P$, is plotted as a function of the level of silica production (Fig. 4A), the data points fall along a hyperbolic curve reminiscent of that obtained when the *f*-ratio for N use is plotted as a function of the level of primary productivity (Eppley and Peterson 1979). The $1 - \int D : \int P$ values range from a minimum of ~0.3 for oligotrophic regions with silica production rates <5 mmol Si m^{-2} d^{-1} and rise to a maximum of ~0.9 for regions with mean silica production rates greater than ~40 mmol Si m^{-2} d^{-1} (Fig. 4A). The curve drawn on Fig. 4A is a rectangular hyperbola fit to the data. A zero intercept was chosen based on the assumption that as silica production approaches zero the fraction of silica production supported by new silicic acid (i.e., $1 - \int D : \int P$) must also be zero. The choice of a rectangular hyperbola is arbitrary, but the equation fits the data well with an R^2 of 0.70, which is significant at the $p < 0.05$ level. The fit is remarkable considering the diversity of habitats represented and the small size of the global data set. This analysis suggests that it might be possible to predict the mean level of silica recycling in a system based on its overall level of silica production.

Figure 4A conceals a great deal of temporal variability. The data points for the ACC and a Gulf Stream warm-core ring each represent means of the results from multiple cruises that sampled during diatom blooms, as well as before and/or after diatom blooms. When the data from each cruise are plotted separately, they separate into two groups that fall along two straight lines, rather than following along a single hyperbolic curve (Fig. 4B). The data were fit simultaneously to two parallel lines using linear regression (Neter and Wasserman 1974), yielding an R^2 value of 0.95 that is significant at the $p < 0.01$ level. One line of the pair encompasses data with relatively high values of $1 - \int D : \int P$ (ca. 0.7–0.9) and

represents cruises that generally sampled diatom blooms or highly productive waters. In these cases, very little of the silica production was supported by silica dissolution in the euphotic zone. The majority of the remaining data are from expeditions that sampled nonbloom conditions. These periods were characterized by low values of $1 - \int D : \int P$ between ~0.3 and 0.4, indicating that 60–70% of the silica produced under nonbloom conditions was redissolving in the euphotic zone. The sole exception to these trends occurs in the case of the relative high value of $1 - \int D : \int P$ observed in the ACC under prebloom conditions by Nelson and Gordon (1982). The relatively high value that they observed could have been a result of the onset of the spring bloom during the study. The study occurred in early spring when biomass levels were still low; however, specific rates of silica production were in the same range as those measured during an intense summer diatom bloom in the Antarctic Polar Front by Brzezinski et al. (2001), and siliceous biomass in the Nelson and Gordon (1982) study was noticeably concentrated in the upper 10–20 m. Nelson and Gordon might have sampled the onset of the bloom when values of $1 - \int D : \int P$ would be expected to be increasing.

The overall impression left by Fig. 4 is that there is a shift from silica dissolution supporting a small fraction of gross silica production during diatom blooms, irrespective of the level of silica production within a given bloom, to silica dissolution supporting the majority of gross silica production during nonbloom periods when silica production is low. Because this trend holds for environments as different as the Sargasso Sea and the Antarctic Polar Front, it might be applicable to a wide range of marine habitats. This analysis supports the hypothesis that there is a seasonal shift in the character of the silica cycle, from silica behaving mainly like a new nutrient during blooms to one behaving more like a regenerated nutrient afterwards (Brzezinski and Nelson 1989).

Although a low $\int D : \int P$ during blooms and a high $\int D : \int P$ during nonbloom periods could have some broad application, there does not appear to be a simple mechanism underlying the transition from low $\int D : \int P$ during blooms to high $\int D : \int P$ during nonbloom periods. One might predict a priori that $\int D : \int P$ would increase following blooms because of an increase in the relative proportion of detrital biogenic silica in the water column from cell death and grazing following bloom events. The frustules of living diatoms are protected from dissolution by their organic coating (Kamatani 1982), and degradation of this coating accelerates dissolution (Kamatani 1982; Bidle and Azam 1999, 2001; Bidle et al. 2003). It is reasonable to hypothesize that more biogenic silica would be in the detrital fraction during nonbloom periods when diatom growth rates are low relative to grazing and bacterial processes. This simple explanation is not consistent with the available data. For the two studies where a seasonal change in the $\int D : \int P$ ratio has been observed, the factors that caused the observed shift in the ratio were different in each study. In the case of Gulf Stream warm-core ring 82B, the increase in $\int D : \int P$ was due mainly to an increase in dissolution rates following the demise of the bloom (Brzezinski and Nelson 1989), but in the case of the Antarctic Polar Front, the increase in $\int D : \int P$ following the bloom was caused by a sharp decline in silica production

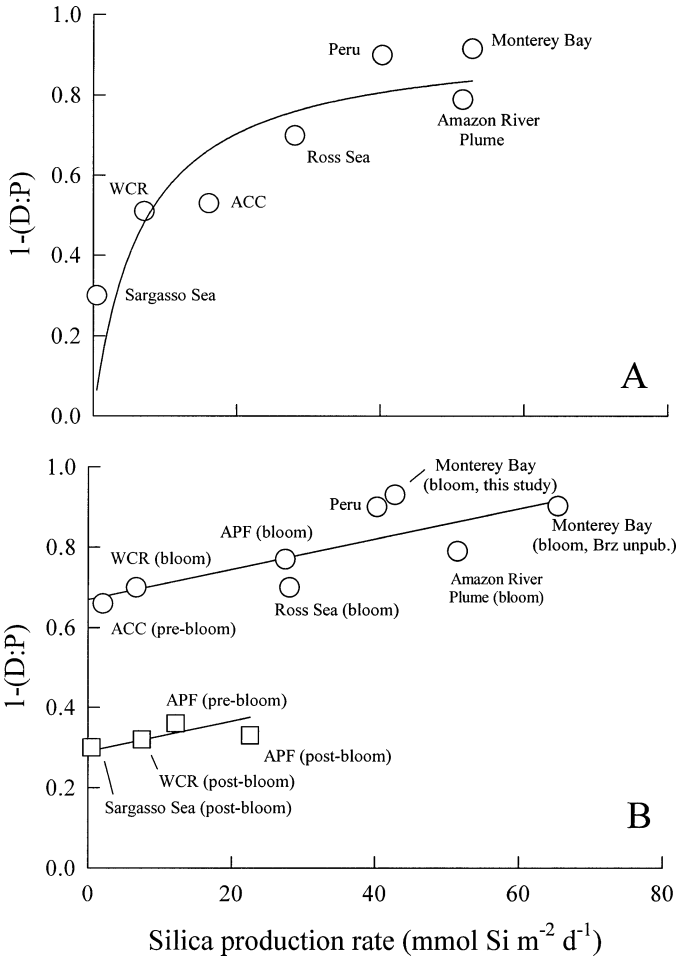

Fig. 4. (A) The fraction of water column silica production supported by new silicic acid ($1 - \int D : \int P$) as a function of the mean silica production rate in different regions of the global ocean. Data from all cruises within a given region were used to calculate each mean silica production rate and mean value of $1 - (\int D : \int P)$. The labels correspond to the following studies: Monterey Bay (this study; Brzezinski unpubl.); Amazon River Plume (DeMaster et al. 1991), excluding data from stations inside of the turbid river plume; Peru coastal upwelling zone (Nelson et al. 1981); ACC, Antarctic Circumpolar Current (Nelson and Gordon 1982; Brzezinski et al. 2001); WCR, Gulf Stream warm-core ring 82-B (Brzezinski and Nelson 1989); Sargasso Sea, data from the Bermuda Atlantic Time Series (BATS) site (Brzezinski and Nelson 1995; Nelson and Brzezinski 1997); Ross Sea, only data in the euphotic zone (surface to 1.0% E_o) considered (Nelson et al. 1991). The curve plotted in panel A represents a rectangular hyperbola fit to all data points. The equation for the line is $1 - \int D : \int P = 0.944 \times \rho/(6.80 + \rho)$, $R^2 = 0.70$ ($p < 0.05$), where ρ is the mean regional silica production rate. (B) Data from panel A plotted with each cruise represented as a separate data point. Where possible, each cruise is designated as having sampled bloom, prebloom, postbloom, or nonbloom conditions on the basis of the descriptions provided in the original manuscripts for each study. The data points fall into two groups: those representing data from blooms or productive waters (circles) and those that sampled pre- or postbloom conditions (squares). Lines shown are parallel regression lines fit simultaneously to the two groups of points ($1 - \int D : \int P = 0.0037\rho + 0.29$, $1 - \int D : \int P = 0.0037\rho + 0.67$; $R^2 = 0.95$, $p < 0.01$). Note that the data from the ACC in panel A is subdivided into the ACC (Nelson and Gordon 1982) and the APF (Antarctic Polar Front, Brzezinski et al. 2001) in panel B.

with silica dissolution rates remaining relatively constant (Brzezinski et al. 2001). Although we cannot explain why these differences exist at the present time, elucidating the underlying mechanisms will be required if we are to develop a predictive capability to understand seasonal changes in silica cycling.

No study of silica cycling has followed the termination of a diatom bloom in a coastal system, making it difficult to ascertain whether seasonal patterns in $\int D:\int P$ occur in nearshore environments. We sampled several stations in Monterey Bay with high biomass and low ambient $[Si(OH)_4]$, implying that the bloom sampled at these locations was nearing nutrient depletion, but there was no discernible increase in $\int D:\int P$ at those stations. Our highest $\int D:\int P$, 0.607, occurred at a station at the edge of the upwelling plume (Sta. 6; *see* Figs. 1, 2). This station had very low siliceous biomass and low $[Si(OH)_4]$, which can be interpreted as representing the terminal phases of a diatom bloom after most of the biomass has been exported to depth. A switch to high $\int D:\int P$ might be common at the end of diatom blooms irrespective of the environment, but that conclusion must be supported by considerably more data before being accepted as a generality.

The values of V_{dis} that we measured in Monterey Bay (Table 1) were generally less than the values observed in exponential cultures of diatoms by Nelson et al. (1976), suggesting that very little detrital silica was present in the upper water column during our study. Interestingly, the D : P ratios calculated for the diatoms cultured by Nelson et al. (1976) are not very different from those we observed in Monterey Bay. Using their data, we calculate a D : P of 0.090 and 0.069 for exponentially growing cultures of *Thalassiosira weissflogii* and *Thalassiosira psuedonana*, respectively. Those values are indistinguishable from the mean $\int D:\int P$ value of 0.075 observed for natural assemblages in this study and are close to the values for the Peru upwelling system, the nonturbid waters of the Amazon River plume, and Monterey Bay (Fig. 4). It is unclear whether such low D : P ratios represent true silica dissolution because the isotope dilution method used in both the field and laboratory studies considered here cannot distinguish between the dissolution of silica and the loss of internal pools of dissolved Si that were present in diatom cells before the seawater was augmented with tracer. Significant leakage of the internal dissolved Si pools of diatoms does occur (Sullivan and Volcani 1981; Hildebrand 2000; Martin-Jezequel et al. 2000), but the extent to which this contributes to dissolution rate estimates in the sea using isotope dilution techniques is unknown. A D : P ratio for healthy diatoms of 0.05–0.1 might represent the minimum value that can be expected in the sea. Blooms with such low D : P ratios thus have the potential to export a large fraction of $bSiO_2$ production from the euphotic zone with minimal losses from dissolution.

If low $\int D:\int P$ ratios are characteristic of diatom blooms in general, how do we reconcile that idea with estimates that the global ocean mean $\int D:\int P$ value is 0.5 or greater in the upper 200 m of the ocean (Nelson et al. 1995; Gnanadesikan 1999; Gnanadesikan and Toggweiler 1999)? Resolution likely involves both temporal and spatial effects. Annual silica production cycles have been measured in only four regions: the Sargasso Sea (Brzezinski and Nelson 1995; Nelson and Brzezinski 1997), the Ross Sea (Nelson et al. 1996), the Antarctic Polar Front (Brzezinski et al. 2001), and the Santa Barbara Channel (Shipe and Brzezinski 2001). A consistent feature of these studies is that diatom blooms occupy a given locality for a relatively short time but account for a disproportionately large fraction of annual silica production and export. In the two studies where dissolution rates have been measured during and after a diatom bloom, $\int D:\int P$ rose significantly after each bloom to a value of >0.6 (Brzezinski and Nelson 1989; Brzezinski et al. 2001). Thus, low $\int D:\int P$ during diatom blooms might be offset by $\int D:\int P > 0.5$ during nonbloom periods, to yield an annual mean of 0.5–0.6 for the global ocean.

Another factor leading to the apparent high global mean $\int D:\int P$ ratio is what appears to be a difference in the balance between silica production and dissolution between the oligotrophic open sea and the more productive regions of the ocean. The oligotrophic midocean gyres have a $\int D:\int P$ of 0.8 during most of the year, and diatom blooms are small in magnitude and infrequent (Brzezinski and Nelson 1995; Nelson and Brzezinski 1997). Nelson et al. (1995) estimated that the midocean gyres account for between 9 and 11% of global silica production, largely on the basis of data from the Sargasso Sea. Subsequent measurements in the Pacific indicated much higher rates, implying that the contribution of the gyres to global silica production is 20–30% (Brzezinski et al. 1998). Here, we assume a contribution of the midocean gyres to global silica production of 25% and an annual $\int D:\int P$ of 0.8 for these regions. To achieve a global marine $\int D:\int P$ of 0.60, the mean annualized $\int D:\int P$ for the remaining 75% of global silica production is 0.53, which is a composite of the $\int D:\int P$ values of 0.6 or greater that have been recorded following blooms and low $\int D:\int P$ values recorded during blooms. Given that diatom blooms account for about 40% of annual silica production in those systems where their contribution to annual silica production has been quantified (Nelson and Brzezinski 1997; Brzezinski et al. 2001; Shipe and Brzezinski 2001), a mean nonbloom $\int D:\int P$ of 0.8 and an annual mean $\int D:\int P$ of 0.53 yields an estimate for the $\int D:\int P$ during blooms of 0.13, which is close to what we observed in the bloom in Monterey Bay. These calculations are very sensitive to the value of $\int D:\int P$ for nonbloom conditions. For example, if we use the nonbloom $\int D:\int P$ of 0.7 implied by Fig. 4B, the $\int D:\int P$ during blooms is 0.28. That value is about double the value of 0.13 obtained above assuming a nonbloom $\int D:\int P$ of 0.8, but it is consistent with the mean $\int D:\int P$ for blooms illustrated in Fig. 4. Such calculations are necessarily crude because of the paucity of measured silica dissolution rates in the surface ocean, but they illustrate that the concept that diatom blooms with very low $\int D:\int P$ account for the majority of silica export in the sea is not at odds with a global annual mean $\int D:\int P$ value of 0.5–0.6. Confirmation of this concept will require quantification of the annual cycle in $\int D:\int P$ for several ocean regions, but independent results from measurements of export from a variety of studies confirm the importance of episodic events, and diatom blooms in particular, to the net export of materials from surface waters (Buesseler 1998).

References

BIDLE, K. D., AND F. AZAM. 1999. Accelerated dissolution of diatom silica by marine bacterial assemblages. Nature **397:** 508–512.

———, AND ———. 2001. Bacterial control of silicon regeneration from diatom detritus; significance of bacterial ectohydrolases and species identity. Limnol. Oceanogr. **46:** 1606–1623.

———, M. A. BRZEZINSKI, R. A. LONG, J. JONES, AND F. AZAM. 2002. Diminished efficiency in the oceanic silica pump caused by bacteria-mediated silica dissolution. Limnol. Oceanogr. **48:** 1855–1868.

BRULAND, K. W., E. L. RUE, AND G. J. SMITH. 2001. Iron and macronutrients in California coastal upwelling regions: Implications for diatom blooms. Limnol. Oceanogr. **46:** 1661–1674.

BRZEZINSKI, M. A., AND D. M. NELSON. 1986. A solvent extraction method for the colorimetric determination of nanomolar concentrations of silicic acid in seawater. Mar. Chem. **19:** 139–151.

———, AND D. M. NELSON. 1989. Seasonal changes in the silicon cycle within a Gulf Stream warm-core ring. Deep-Sea Res. **36:** 1009–1030.

———, AND ———. 1995. The annual silica cycle in the Sargasso Sea near Bermuda. Deep-Sea Res. I **42:** 1215–1237.

———, AND D. R. PHILLIPS. 1997. Evaluation of ^{32}Si as a tracer for measuring silica production rates in marine waters. Limnol. Oceanogr. **42:** 856–865.

———, ———, F. P. CHAVEZ, G. E. FRIEDERICH, AND R. C. DUGDALE. 1997. Silica production in the Monterey, California upwelling system. Limnol. Oceanogr. **42:** 1694–1705.

———, T. A. VILLAREAL, AND F. LIPSCHULTZ. 1998. Silica production and the contribution of diatoms to new and primary production in the central North Pacific. Mar. Ecol. Prog. Ser. **167:** 89–104.

———, D. M. NELSON, V. M. FRANCK, AND D. E. SIGMON. 2001. Silicon dynamics within an intense open-ocean diatom bloom in the Pacific sector of the Southern Ocean. Deep-Sea Res. II **48:** 3997–4018.

BUESSELER, K. O. 1998. The decoupling of production and particle export in the surface ocean. Glob. Biogeochem. Cycles **12:** 297–310.

DEMASTER, D. J., B. A. MCKEE, W. S. MOORE, AND D. M. NELSON. 1991. Geochemical processes ocurring in the waters at the Amazon River/ocean boundary. Oceangraphy **4:** 15–20.

DUGDALE, R. C., AND F. P. WILKERSON. 1989. Regional perspectives in global new production, p. 289–308. *In* M. M. Denis [ed.], Oceanologie actualite et prospective. Centre d'Oceanologie de Marseille, France.

———, AND ———. 1998. Silicate regulation of new production in the equatorial Pacific upwelling. Nature **391:** 270–273.

———, ———, AND H. J. MINAS. 1995. The role of the silicate pump in driving new production. Deep-Sea Res. I **42:** 697–719.

———, R. T. BARBER, F. CHAI, T. H. PENG, AND F. P. WILKERSON. 2002. 1-D ecosystem model of the equatorial Pacific upwelling system, part II: Sensitivity analysis and comparison with JGOFS EqPac data. Deep-Sea Res. II **49:** 2713–2745.

EPPLEY, R. W., AND B. J. PETERSON. 1979. Particulate organic matter flux and planktonic new production in the deep ocean. Nature **282:** 677–680.

GNANADESIKAN, A. 1999. A global model of silicon cycling: Sensitivity to eddy parameterization and dissolution. Glob. Biogeochem. Cycles **13:** 199–220.

———, AND J. R. TOGGWEILER. 1999. Constraints placed by silicon cycling on vertical exchange in general circulation models. Geophys. Res. Lett. **26:** 1865–1868.

HILDEBRAND, M. 2000. Silicic acid transport and its control during cell wall silicification in diatoms, p. 171–188. *In* E. Baeuerlein [ed.], Biomineralization: From biology to biotechnology and medical application. Wiley.

HURD, D. C. 1972. Factors affecting the solution rate of biogenic opal in seawater. Earth Planet. Lett. **15:** 411–417.

———, AND S. BIRDWHISTELL. 1983. On producing a general model for biogenic silica dissolution. Am. J. Sci. **283:** 1–28.

KAMATANI, A. 1982. Dissolution rates of silica from diatoms decomposing at various temperatures. Mar. Biol. **68:** 91–96.

———, AND J. P. RILEY. 1979. Rate of dissolution of diatom silica walls in seawater. Mar. Biol. **55:** 29–35.

KARL, D. M., AND G. TIEN. 1992. MAGIC: A sensitive and precise method for measuring dissolved phosphorus in aquatic environments. Limnol. Oceanogr. **37:** 105–116.

KUDELA, R. M., AND R. C. DUGDALE. 2000. Nutrient regulation of primary productivity in Monterey Bay, California. Deep-Sea Res. II **47:** 1023–1053.

MARTIN-JEZEQUEL, V., M. HILDEBRAND, AND M. A. BRZEZINSKI. 2000. Silicon metabolism in diatoms: Implications for growth. J. Phycol. **36:** 821–840.

NELSON, D. M., AND M. A. BRZEZINSKI. 1997. Diatom growth and productivity in an oligotrophic midocean gyre: A 3-yr record from the Sargasso Sea near Bermuda. Limnol. Oceanogr. **42:** 473–486.

———, AND J. J. GOERING. 1977. Near-surface silica dissolution in the upwelling region off northwest Africa. Deep-Sea Res. **24:** 65–73.

———, AND L. I. GORDON. 1982. Production and pelagic dissolution of biogenic silica in the Southern Ocean. Cosmochim. Acta **46:** 491–500.

———, S. S. GOERING, S. S. KILHAM, AND R. R. L. GUILLARD. 1976. Kinetics of silicic acid uptake and rates of silica dissolution in the marine diatom *Thalassiosira pseudonana.* J. Phycol. **12:** 246–252.

———, J. J. GOERING, AND D. W. BOISSEAU. 1981. Consumption and regeneration of silicic acid in three coastal upwelling systems, p. 242–256. *In* F. A. Richards [ed.], Coastal upwelling. American Geophysical Union.

———, J. A. AHERN, AND L. J. HERLIHY. 1991. Cycling of biogenic silica within the upper water column of the Ross Sea. Mar. Chem. **35:** 461–476.

———, P. TRÉGUER, M. A. BRZEZINSKI, A. LEYNAERT, AND B. QUÉGUINER. 1995. Production and dissolution of biogenic silica in the ocean: Revised global estimates, comparison with regional data and relationship to biogenic sedimentation. Glob. Biogeochem. Cycles **9:** 359–372.

———, D. J. DEMASTER, R. B. DUNBAR, AND W. O. SMITH JR. 1996. Cycling of organic carbon and biogenic silica in the Southern Ocean: Estimates of water-column and sedimentary fluxes on the Ross Sea continental shelf. J. Geophys. Res. **101:** 18,519–18,532.

NETER, J., AND W. WASSERMAN. 1974. Applied linear statistical models. Richard D. Irwin.

SHIPE, R. F., AND M. A. BRZEZINSKI. 2001. A time-series study of silica production and flux in an eastern boundary region: Santa Barbara Basin, California. Glob. Biogeochem. Cycles **15:** 517–531.

SULLIVAN, C. W., AND B. E. VOLCANI. 1981. Silicon in the cellular metabolism of diatoms, p. 15–42. *In* T. L. Simpson and B. E. Volcani [eds.], Silicon and siliceous structures in biological sytems. Springer-Verlag.

Received: 6 May 2002
Accepted: 11 November 2002
Amended: 14 February 2003